Modeling the Organic Nitrate Yields in the Reaction of Alkyl Peroxy Radicals with Nitric Oxide. 2. Reaction Simulations

John R. Barker,*,†,‡ Lawrence L. Lohr,‡ Robert M. Shroll,†,# and Susan Reading†

Department of Atmospheric, Oceanic, and Space Sciences, University of Michigan, Ann Arbor, Michigan 48109-2143, and Department of Chemistry, University of Michigan, Ann Arbor, Michigan 48109-1055

Received: March 12, 2003; In Final Form: June 20, 2003

Master equation calculations are used to model gas-phase literature experimental data for alkyl nitrate formation via the following reaction system of reversible reactions: (1) $RO_2 + NO \leftrightarrow ROONO$, (2) $ROONO \leftrightarrow RO + NO_2$, (3) $ROONO \leftrightarrow RONO_2$, and (4) $RONO_2 \leftrightarrow RO + NO_2$ for R = CH_3, *i*-C_3H_7, and 2-C_5H_{11}. The structures and thermochemistry of the stable species are based on electronic structure calculations described in the preceding companion paper in this issue (Lohr et al. *J. Phys. Chem. A* **2003**, *107*, xxx−xxx). Literature data for recombination rate constants are used to constrain the model calculations. Several transition state models and a range of energy transfer parameters are investigated. The results for R = CH_3 show that a wide variety of plausible transition state models for k_{-4} gives good agreement with experiment for reaction (−4), because changes in assumed energy transfer parameters can compensate for differences between the transition state models. It is concluded that recombination reactions are good sources of absolute energy transfer parameters only when transition state properties are known with great accuracy. Although satisfactory models are obtained for the individual systems, the parameters cannot be transferred reliably from one system to another. Master equation models can be made to reproduce the experimental 2-pentyl nitrate yields from the title reaction as long as $\langle \Delta E \rangle_{down}$, the average energy transferred in deactivating collisions, is assumed to be surprisingly, and perhaps unphysically, small (∼25 cm^{-1}), regardless of assumptions about the barrier to isomerization reaction 3. Several critical assumptions in the master equation models are examined, but none of them accounts for the small value of $\langle \Delta E \rangle_{down}$. It is concluded that new experiments should be carried out to verify or possibly revise the pressure-dependent alkyl nitrate yield data currently available in the literature.

Introduction

In 1976, Darnall et al.[1] reported that the reaction of alkyl peroxy radicals (RO_2•) with nitric oxide in the gas phase produces not only alkoxy radicals (RO•) and NO_2, but also a significant yield of alkyl nitrates:

$$RO_2\bullet + NO \rightarrow RO\bullet + NO_2 \quad (A)$$

$$\rightarrow MRONO_2 \quad (B)$$

This result is important for understanding the chemistry of the atmosphere, because alkyl nitrates are relatively inert in the troposphere[2] and therefore reaction B is a sink for both RO_2• radicals and NO_2, the direct precursor of ozone in the lower atmosphere. When NO_2 is removed efficiently, less ozone is produced in the photochemical system.

The discovery of reaction B was not only important, but surprising, because to form alkyl nitrates, the O−O bond in the RO_2• radical must be broken and two new O−N bonds must be formed. This gas-phase internal molecular rearrangement requires a three-center cyclic transition state, which is expected to have a high energy barrier to reaction.[3] There is little doubt, however, that nitrates are formed via reaction B, since significant reaction yields have been measured in both static and flowing systems by numerous analytical methods.[2,4,5] The reaction scheme shown in Figure 1 (postulated by Atkinson et al.[6]) is qualitatively consistent with all of the experimental data for R = H, alkyl, and substituted alkyl.

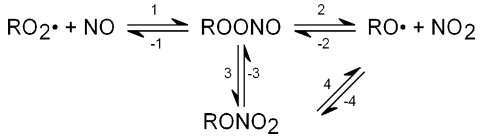

Figure 1. Reaction scheme.

The purpose of the present work is to use reaction Scheme 1 (Figure 1) in a quantitative assessment of alkyl nitrate formation on the basis of master equation models and results from electronic structure calculations. Master equation models are capable of simulating very complex chemical systems and testing for the internal consistency of experimental results. Results from electronic structure calculations are presented in the companion paper in this issue (ref 7), where it is shown that the calculated thermochemical quantities, vibrational frequencies, and molecular structures are in excellent agreement with the available measured values. Zhang et al.[8] reported electronic structure and master equation calculations on nitrites and nitrates formed in the OH + isoprene reaction system that are similar in concept to the present work, but different in detail. Their results, obtained only for room temperature at one atmosphere, are in qualitative agreement with those reported here.

* Address correspondence to this author. E-mail: jrbarker@umich.edu.
† Department of Atmospheric, Oceanic, and Space Sciences.
‡ Department of Chemistry.
# Present Address: Spectral Sciences Inc., 99 South Bedford Street, Suite 7, Burlington MA 01803.

10.1021/jp034638j CCC: $25.00
Published on Web 08/20/2003

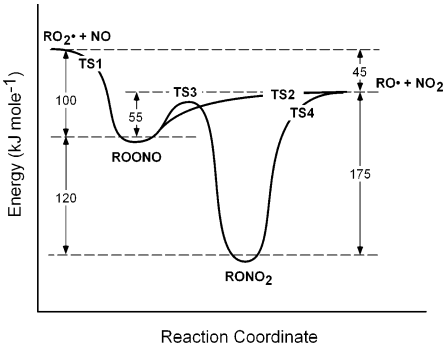

Figure 2. Schematic potential energy surface (transition states are noted; energies[7] expressed in units of kJ mol^{-1}). See Table 1.

In the present paper, the calculated quantities are used in conjunction with experimental kinetics data from the literature to construct detailed master equation models of the reaction systems involving R = CH_3, *i*-C_3H_7, and 2-C_5H_{11}. It is shown below that the master equation models can accurately describe the alkyl nitrate yields, but some of the model parameters are quite surprising, and lead to questions regarding the accuracy of some of the experimental data.

Theoretical Methods. The reaction scheme and the corresponding potential energy surface, shown in Figures 1 and 2, show that this chemical system is a multiwell, multichannel unimolecular reaction system. Since the reaction rates are energy dependent and collisional energy transfer is not perfectly efficient, the system is best treated using master equation techniques. To implement the master equation model, parameters must be assigned for four reversible reactions and for energy transfer involving two chemical species. The numerous parameters were assigned by using conventional unimolecular reaction rate theory, the electronic structure calculations reported in the preceding companion paper in this issue, and ancillary chemical kinetics data from the literature.

Rate Constant Expressions. In principle, each of the rate constants for dissociation and isomerization depends on vibrational energy and angular momentum, as does energy transfer within the two potential wells. In the present work, a one-dimensional (vibrational energy) master equation treatment is employed. The effect of angular momentum on the dissociation reactions is treated using the pseudo-diatomic approximation.[9] The MultiWell software package[10−12] was used for all of the calculations.

Unimolecular reaction rates were calculated using Rice-Ramsperger-Kassal-Marcus (RRKM) theory,[9,13,14] which requires calculation of the sums and densities of internal states for the two potential wells and for the four transition states. The electronic structure calculations from the preceding companion paper in this issue provided normal mode vibrational frequencies and moments of inertial for the two wells. In many cases, inspection of the normal mode motions enabled us to distinguish vibrational modes from the torsional modes, which were treated as hindered internal rotations. In the present work, all of the sums and densities of states are calculated (program DenSum[12]) by "exact counts" (energy grain of 5 or 10 cm^{-1}), using the Beyer−Swinehart algorithm[15] as adapted by Stein and Rabinovitch.[16]

According to RRKM theory,[9,13,14] the energy-dependent specific unimolecular rate constant $k(E)$ is given by

$$k(E) = \left[\frac{m^{\ddagger}}{m}\frac{\sigma_{\mathrm{ext}}}{\sigma_{\mathrm{ext}}^{\ddagger}}\right]\frac{g_{\mathrm{e}}^{\ddagger}}{g_{\mathrm{e}}}\frac{1}{h}\frac{G^{\ddagger}(E-E_0)}{\rho(E)} \qquad (1)$$

where $m^{\ddagger}$ and m are the number of optical isomers, $\sigma_{\mathrm{ext}}^{\ddagger}$ and σ_{ext} are the external rotation symmetry numbers, and $g_{\mathrm{e}}^{\ddagger}$ and g_{e} are the electronic state degeneracies of the transition state and reactant, respectively; h is Planck's constant, $G^{\ddagger}(E-E_0)$ is the sum of states of the transition state, E_0 is the reaction threshold energy, and $\rho(E)$ is the density of states of the reactant molecule. The internal energy E is measured relative to the zero point energy of the reactant molecule and the reaction threshold energy (critical energy) is the difference between the zero point energies of reactant and transition state. Equation 1 was written by assuming that the rotational *external* symmetry numbers, electronic degeneracies, and numbers of optical isomers were *not* used in calculating the sums and densities of states. It is, however, assumed that *internal* rotor symmetry numbers are used explicitly in the sum and density calculations and hence do not appear in eq 1. Note that the quantity set off in square brackets is the reaction path degeneracy.

When the structure of the transition state is not known, it is often convenient to use the inverse Laplace transform (ILT) method described by Forst:[9,17]

$$k(E) = \left[\frac{m^{\ddagger}}{m}\frac{\sigma_{\mathrm{ext}}}{\sigma_{\mathrm{ext}}^{\ddagger}}\right]\frac{g_{\mathrm{e}}^{\ddagger}}{g_{\mathrm{e}}}A_{\infty}\frac{\rho(E-E_{\infty})}{\rho(E)} \qquad (2)$$

where A_∞ and E_∞ are the Arrhenius parameters (corrected for degeneracy factors and symmetry) for the corresponding high-pressure limiting thermal rate constant. For added accuracy near the reaction threshold, E_∞ was replaced in eq 2 by E_0, the threshold energy. This substitution improves the threshold behavior, but introduces a small error in the calculated activation energy at the high-pressure limit.

Centrifugal corrections to the unimolecular rate constants were made according to the pseudo-diatomic model, where the reaction threshold energy at a given temperature is corrected approximately for angular momentum effects by using a threshold energy E_0^{T} given by the following expression:[9]

$$E_0^{\mathrm{T}} = E_0 - k_{\mathrm{B}}T\left\{1 - \frac{I_{2\mathrm{D}}}{I_{2\mathrm{D}}^{\ddagger}}\right\} \qquad (3)$$

where I_{2D} and $I_{2D}^{\ddagger}$ are the moments of inertia for the external two-dimensional (2-D) inactive (adiabatic) rotations of the reactant and of the transition state, respectively, and k_B is Boltzmann's constant. The resulting expression for $k(E)$ corresponds to that given by eq 4.29 in Robinson and Holbrook.[14]

For a thermal distribution, recombination reaction rate constants (k_{rec}) are related to the corresponding unimolecular rate constants (k_{uni}) according to the equilibrium constant (K). Thus, at the high-pressure limit we have the relationship

$$K = \frac{k_{\mathrm{rec}}^{\infty}}{k_{\mathrm{uni}}^{\infty}} \qquad (4)$$

In the present work, equilibrium constants were calculated using the computer code Thermo,[12] which employs conventional statistical mechanics formulas for separable degrees of freedom that include harmonic and anharmonic oscillators, free and hindered internal rotors, and external rotational degrees of freedom.

In recombination reactions, the two reactants come together to form a highly excited adduct, which can redissociate, be collisionally deactivated, and react via other reaction channels. The chemical activation energy distribution[10] describes the

nascent energy distribution of the complex formed in the recombination reaction:

$$y_0^{(ca,i)}(E)dE = \frac{k_i(E)\rho(E)e^{-E/k_BT}dE}{\int_{E_0}^{\infty} k_i(E')\rho(E')e^{-E'/k_BT}dE'} \quad \text{for } E \geq E_0 \tag{5}$$

where $y_0^{(ca,i)}(E)$ is the energy distribution of molecules formed via reaction channel i, which has energy threshold E_0 and specific rate constant $k_i(E)$, $\rho(E)$ is the density of states in the new molecule, and the zero of energy for this equation is at the zero point energy of the newly formed species.

Loose Transition States. For "loose" transition states, in which a chemical bond is greatly elongated, the properties of the transition state depend sensitively on angular momentum and the detailed shape of the interaction potential. In the absence of other information, it is possible to estimate the rate constant by using variational transition state theory with a calculated potential energy surface.[13,18] When the rate constant is known, however, it is more convenient to use a "restricted" Gorin model with a "hindrance parameter" selected to reproduce the known rate constant for the corresponding reverse (recombination) reaction.[3,13,19]

According to the Gorin model,[20] the two molecular fragments rotate independently of one another while separated at the distance corresponding to the centrifugal maximum (r_{max}) of the effective potential of the bond being broken. In the present work, the rotations of both fragments and the overall transition state are treated approximately as symmetric tops. The overall transition state has a 2-D external adiabatic rotation with moment of inertia given by $I_{2D}^{\ddagger} = \mu r^2_{max}$, where μ is the reduced mass of the two fragments, and a 1-D external rotation (the "K-rotor") with moment of inertia I_k. The K-rotor is not adiabatic and is assumed, according to the usual approximation,[13] to mix energy freely with the active vibrations. The internal rotations of fragments A and B are characterized by 2-D rotations with moments of inertia I_a and I_b, respectively, and an internal rotation with reduced moment of inertia I_r. The moments of inertia I_r and I_k are obtained by combining the K-rotors of the individual fragments, as described by Gilbert and Smith.[13]

In the restricted Gorin model,[3,13,19] it is assumed that the two fragments interfere sterically with each another and thus cannot rotate freely. The effect is to reduce the available phase space and hence reduce the sum of states. Operationally, a "hindrance" parameter η is defined,[19] which can vary from zero (free rotation) to unity (completely hindered). The 2-D moments of inertia I_a and I_b are multiplied by the factor $(1 - \eta)^{1/2}$ to obtain the effective 2-D moments of inertia used for calculating the sum of states. These parameters are tabulated for all of the restricted Gorin transition states used in the present work.

In general, the potential function describing the breaking bond is not known and any one of three potential functions is commonly assumed for the bond fission: the Lennard−Jones potential, the Morse potential, or the Varshni potential (see below). The centrifugal maximum is found at the shortest distance with the Varshni potential and at the longest distance with the Lennard−Jones potential. Although the centrifugal maximum is found at different distances with the different assumed potential functions, the resulting thermal rate constants are the same because hindrance parameters must be selected to match the known rate constant. Changes in the hindrance parameter and in r_{max} compensate for each other.

The Lennard-Jones potential is often chosen for its simplicity as well as because it has the long range dependence on r^{-6} expected for many long-range potentials, although it does not describe a chemical bonding interaction very well at short range (near the potential minimum energy). For the Lennard−Jones potential, the moment of inertia for the two-dimensional adiabatic external rotation is given by $I_{2D}^{\ddagger} = \mu r_e^2(6D_e/RT)^{1/3}$, where r_e is the equilibrium bond distance, μ is the reduced mass, and $D_e = D_0 - \Delta E_z$, where D_0 is the bond dissociation enthalpy at 0 K, ΔE_z is the zero point energy difference between products and reactants, and R is the gas law constant.

The Morse oscillator potential describes the short range chemical interactions relatively well, but its long-range behavior is not accurate. The Varshni potential function[21] is a better choice[22,23] because it is more similar to ab initio results reported by Duchovic and Hase[24] for breaking the C−H bond in methane. The Varshni potential function is given by

$$V(r) = D_e\left\{1 - \left(\frac{r_e}{r}\right)\exp[-\beta_v(r^2 - r_e^2)]\right\}^2 - D_e \tag{6a}$$

$$\beta_v = \frac{1}{2r_0}\left[2\pi\nu\sqrt{\frac{\mu}{2D_e}} - \frac{1}{r_0}\right] \tag{6b}$$

where r is the center of mass distance between the two fragments, r_e is the equilibrium distance, D_e is the dissociation energy, ν is the frequency, and μ is the reduced mass. In the present work, the centrifugal maximum supported by the Varshni potential is found by (a) identifying a vibrational frequency corresponding to the breaking bond, (b) finding D_e (see above), and (c) finding the maximum in the effective potential by the secant method. From r_m, the moment of inertia of the 2-D adiabatic external rotation can be calculated: $I_{2D}^{\ddagger} = \mu r_m^2$.

Model Parameters and Constraints. *Stable Species.* The relative energies of stable species (RO•, RO_2•, ROONO, and $RONO_2$) were calculated and discussed in the preceding companion paper in this issue.[7] In the present work, we adopted the specific calculated thermochemistry for R = methyl and the generic alkyl thermochemistry for R = *i*-propyl and 2-pentyl. Literature values were used for the molecular properties of NO and NO_2.[25,26] All of the parameters are presented in Tables 1 and 2, and in the Supporting Information.

RO_2• + NO Reaction. Reaction rate constants for reaction A are known for many alkyl groups.[5,27−30] At low pressures, the reaction produces RO• + NO_2 essentially exclusively because

TABLE 1: Thermochemistry[a] for R ≥ CH_3

reaction	ΔH_r (0 K), kJ mol^{-1}
RO + NO_2 → RO_2 + NO	45
$RONO_2$ → ROONO	120
$RONO_2$ → RO + NO_2	175
ROONO → RO + NO_2	55

[a] Companion paper, ref 7.

TABLE 2: Parameters for Stable Molecular Species

	I_{2D}/amu Å^2	I_K/amu Å^2	symmetry	g_e	m	σ/Å[a]	ϵ/k (K)[a]
CH_3OONO	185	23.6	1	1	2	4.3	484
CH_3ONO_2	127	46.5	1	1	2	4.3	484
i-C_3H_7OONO	334	99.0	1	1	2	5.1	486
i-$C_3H_7ONO_2$	308	98.6	1	1	2	5.1	486
2-$C_5H_{11}OONO$	603	238	1	1	2	5.8	517
2-$C_5H_{11}ONO_2$	637	193	1	1	2	5.8	517
Ar						3.47[69]	114[69]
N_2						3.74[69]	82[69]

[a] Lennard−Jones parameters calculated by the method described in the text, unless otherwise noted.

TABLE 3: Restricted Gorin Models for R = CH_3 at 300 K (endothermic reaction direction)

	Varshni potential			L−J potential		
	TS-1	TS-2	TS-4	TS-1	TS-2	TS-4
I_{2D}/amu Å^2	372	356	463	1208	1009	993
I_K/amu Å^2	8.40	5.30	43.0	8.40	5.30	43.0
I_r/amu Å^2		1.265 (3)	2.97 (6)		1.265 (3)	2.97 (6)
I_a/amu Å^2	46.665	18.13	18.13	46.665	18.13	18.13
I_b/amu Å^2	9.84	39.75	9.11	9.84	39.75	9.11
$(1-\eta)^{1/2}$	0.276	0.244	0.255	0.153	0.145	0.174
symmetry	1	1	1	1	1	1
elec. degen.	1	1	1	1	1	1
opt. isomers	2	2	2	2	2	2
E_0/kJ mol^{-1}	98.8	50.5	173.5	98.8	50.5	173.5
E_{0r}/kJ mol^{-1}	85.2	39.5	156.7	96.3	48.2	167.0
k_∞(297 K)/s^{-1}	3.0×10^{-2}	1.4×10^{7}	9.5×10-^{15}	3.0×10^{-2}	1.4×10^{7}	9.5×10^{-15}
A_∞/s^{-1}	1.58×10^{16}	1.80×10^{16}	1.18×10^{17}	1.59×10^{16}	1.80×10^{16}	1.18×10^{17}
E_∞/kJ mol^{-1}	100.8	51.8	176.7	100.8	51.8	176.8

TABLE 4: ILT Models for R = CH_3 at 300 K (endothermic reaction direction)

	TS-1	TS-2	TS-4
I_{2D}/amu Å^2	1208	1009	993
A_∞/s^{-1}	6.9×10^{15}	1.0×10^{16}	2.9×10^{16}
E_0/kJ mol^{-1}	98.8	50.5	173.5

highly excited ROONO* is not easily stabilized by collisions, and the dissociation reaction is very fast. At higher pressures, excited $RONO_2$* can be stabilized, but the yields are low. Accordingly, the experimental data for the reaction rate constant show little or no pressure dependence. In constructing the master equation model, we assumed that the rate constant k_A can be identified with rate constant k_1^∞ at the high-pressure limit. We used this value for k_1^∞ and the equilibrium constant to obtain k_{-1}^∞.

RO• + NO_2 Reaction. Reaction rate constants for the reaction of RO• + NO_2 have been measured near the high-pressure limit for many alkoxy radicals, and in the falloff for R = methyl.[27−31] The rate constants that have been measured for the loss of RO• radicals presumably correspond to the sum of the rate constants for reactions (−2) and (−4). Since no information is available concerning the relative rate constants for the two reactions, we assumed that addition of RO• to each atom in NO_2 is equally probable. Therefore, the rate of reaction (−2) is assumed to be twice that of reaction (−4). This assumption is generally consistent with the relative yields of HOONO and $HONO_2$ produced in the OH + NO_2 reaction,[32] which were subsequently modeled by Golden et al.[33] Rate constants for the reverse reactions were calculated by using the equilibrium constant, according to eq 4. The resulting high-pressure limit rate constants are listed in Tables 3−6.

For most of the simulations, we used a restricted Gorin model that consisted of the vibrational frequencies of free RO• radicals and NO_2 molecules, as well as a free internal rotation with moment of inertia I_r (see Gilbert and Smith[13]) and two 2-D rotors (two-dimensional rotors) with moments of inertia $I^\ddagger_{RO} = (1-\eta)^{1/2} I_{RO}$, and $I^\ddagger_{NO_2} = (1-\eta)^{1/2} I_{NO_2}$, where η is the hindrance parameter, and I_i (i = RO•, NO_2) is the moment of inertia for the 2-D rotation for torsional rocking of the individual fragment in the transition state. Values for I_i (i = RO•,NO_2), which were chosen in the usual way,[34] are summarized in Tables 3, 5, and 6. The external rotations of the transition state were treated in the usual way: the "K-rotor", whose energy is not conserved, was included with the other active internal degrees of freedom in the sums of states calculation and the 2-D adiabatic rotations were used to make the centrifugal corrections described above.

CH_3O• + NO_2 Falloff. For R = methyl, rate constants for loss of CH_3O• have been measured as a function of pressure and temperature.[31,35−37] The resulting falloff data provide information about energy transfer and the loose transition state model for the recombination reaction. To investigate this aspect, reaction simulations were carried out using four distinct models for $k(E)$: (a) a restricted Gorin transition state model based on the L−J potential, (b) a restricted Gorin transition state model based on the Varshni potential, (c) Forst's ILT method, including centrifugal corrections (based on L−J model), and (d) Forst's ILT model with no centrifugal corrections (i.e., assuming $I^\ddagger_{2D}$ for the transition state is the same as I_{2D} for the molecule CH_3-ONO_2).

Restricted Gorin models were constructed as described above. We used the assumed thermochemistry, the calculated molecular

TABLE 5: Model Parameters for R = *i*-C_3H_7 (endothermic reaction direction)

	TS-1	TS-2	TS-3	TS-4
I_{2D}/amu Å^2	2139	1784	384	2338
I_K/amu Å^2	76.0	107		144
symmetry	1	1	1	1
elec. degen.	1	1	1	1
opt. isomers	2	2	2	2
I_r/amu Å^2		2.05 (1)		28.8 (2)
I_a/amu Å^2	127.6	58.8		58.8
I_b/amu Å^2	9.84	39.75		9.11
$(1-\eta)^{1/2}$	0.266	0.330		0.252
E_0/kJ mol^{-1}	100	55	varied	175
E_{0r}/kJ mol^{-1}	86.7	44.3	varied	158.8
k_∞(297 K)/s^{-1}	8.2×10^{-2}	3.8×10^{7}	varied	7.0×10^{-14}
A_∞/s^{-1}	8.03×10^{16}	2.72×10^{17}	varied	1.43×10^{18}
E_∞/kJ mol^{-1}	101.9	55.8	varied	177.4

TABLE 6: Model Parameters for R = 2-C_5H_{11} (endothermic reaction direction)

		TS-1	TS-2	TS-3	TS-4
I_{2D}/amu Å^2	284 K	3976	3379	1236	5220
	300 K	3862	3283	1236	5125
	326 K	3757	3193	1236	4985
I_K/amu Å^2		119	66		104
symmetry		1	1	1	1
elec. degen.		1	1	1	1
opt. isomers		2	2	2	2
I_r/amu Å^2			2.02 (1)		24.5 (2)
I_a/amu Å^2		371.1	313.9		313.9
I_b/amu Å^2		9.84	39.75		9.11
$(1-\eta)^{1/2}$	284 K	0.165	0.180		0.120
	300 K	0.159	0.177		0.117
	326 K	0.151	0.173		0.114
E_0/kJ mol^{-1}		100	55	varied	175
E_{0r}/kJ mol^{-1}		86.52	43.92	varied	157.4
k_∞(300 K)/s^{-1}		9.4×10^{-2}	4.5×10^{7}	varied	6.8×10^{-14}
A_∞/s^{-1}		4.66×10^{16}	2.13×10^{17}	varied	4.85×10^{17}
E_∞/kJ mol^{-1}		101.6	55.6	varied	177

properties, the distance of the centrifugal maximum, and then we adjusted the hindrance parameter to match the experimental value of k_{-1}^{∞} reported by Wollenhaupt and Crowley.[31] For inverse Laplace transform (ILT) models, we used the assumed thermochemistry and empirically adjusted A_{∞} to obtain agreement with the experimental value of k_1^{∞} at each temperature. The resulting parameters are summarized in Tables 3 and 4.

The L−J potential gives a much larger value for r_{max} (and corresponding moment of inertia) than the relatively tight Varshni potential. The ILT models are also plausible, but they are based on an entirely different assumption. The simulations with, and without, centrifugal corrections helps to show how centrifugal corrections affect the quantitative results.

ROONO → RONO$_2$ Isomerization Reaction. The evidence for the existence of this reaction is very strong, since alkyl nitrates have been measured in many systems, but the properties of the transition state are not known well. Most electronic structure calculations on these systems have found isomerization transition states that are very high in energy, making them energetically inaccessible under ordinary conditions.[38] Recently, Dixon et al.[39] reported finding in the HNO_3 system a plausible transition state with an energy near the HOONO → HO• + NO_2 dissociation limit and a structure that resembles a loosely bound complex between HO• and NO_2. Another recent report[40] for R = H places the barrier height about 22 kJ mol^{-1} above the RO• + NO_2 asymptote. Recently, Ellison et al.[41] reported finding a transition state for R = CH_3 that appears to be "tighter" and at a substantially higher energy (near the energy of RO_2• + NO) than that of Dixon et al.

In the present work, analogous transition states are presumed to exist in the RNO_3 systems, but their properties are not known with any certainty. It is possible that the transition state energies may be found near the RO• + NO_2 energy, as in the HNO_3 system, but it is also possible that inductive effects could lower the isomerization energy barrier substantially. Thus a wide range of possible energy barriers is investigated. In the following, it is arbitrarily assumed that the energy barrier can range from 20 kJ mol^{-1} up to a "high" barrier that is 2.5 kJ mol^{-1} ($\sim k_B T$ at 300 K) below the energy of RO• + NO_2.

For the purpose of the present simulations, the ILT method is used to estimate $k(E)$ for a range of assumed isomerization energy barriers and corresponding A-factors. The purpose is to determine whether the parameters are significantly constrained by the data. It is shown below that a very wide range of parameters is consistent with the data and no unique model can be identified.

Energy Transfer. Accurate energy transfer parameters are scarce and only have been measured by nonchemical means for a few species.[42] Since the present system includes internal rotors, we expect it to have energy transfer parameters that are more similar to those of toluene, rather than benzene (for example). For present purposes, the conventional exponential model for collision step size distribution is assumed

$$P(E',E) = \frac{1}{N(E)} \exp\left[\frac{-(E-E')}{\alpha(E)}\right] \quad \text{for } (E-E') \geq 0 \quad (7)$$

where $P(E',E)$ is the probability density for energy transfer from vibrational energy E to energy E' in a deactivation step, $N(E)$ is a normalization factor, and the energy transfer $\alpha(E)$ is approximately a linear function of internal energy and is almost identical to the average energy transferred in deactivating collisions (i.e., $\langle \Delta E \rangle_{down}$). For single-channel reactions, it makes little quantitative difference in reaction simulations whether $\alpha(E)$ is treated as a constant, or as a function of energy. Although the present system involves two wells and multiple channels, only one reaction channel is susceptible to collisions (see below), and we minimized the number of adjustable parameters by assuming that $\alpha(E)$ is independent of energy.

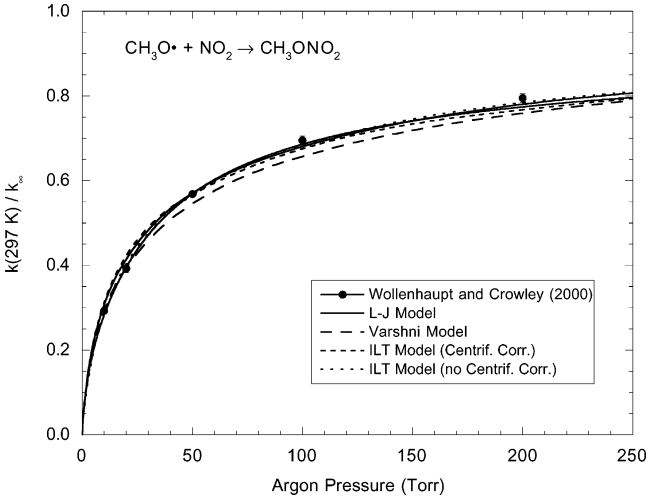

Figure 3. Falloff curve for the reaction of CH_3O• + NO_2 in argon at 297 K. Experimental data (points) and $k_{\infty}(297\ K) = 1.9 \times 10^{-11}$ cm^3 s^{-1} are from Wollenhaupt and Crowley;[31] lines are model calculations (see Tables 3 and 4).

Collision frequencies were calculated by assuming Lennard−Jones intermolecular potentials. The Lennard−Jones parameters for $RONO_2$ and ROONO were estimated according to the methods of Mourits and Rummens,[43] who recommend for polar compounds the average of the results obtained using the methods of Stiel and Thodos[44] and of Halkiadakis and Bowrey.[45] Both methods employ a correspondence principle relating the Lennard−Jones parameters to the critical pressure, critical volume, and critical temperature, which were calculated using the Joback and Reid method[46] as implemented in Chem-3D Pro v.5 (Cambridge Software). The Lennard−Jones parameters and collision rate constants are summarized in the tables.

Model Calculations and Results

CH_3O• + NO_2 → Products. The rate constant for this reaction exhibits falloff at pressures less than one atmosphere of helium or argon.[31,35−37] For simplicity, the simulations carried out here are of the recent study by Wollenhaupt and Crowley,[31] which is in excellent agreement with the earlier studies. As mentioned above, four distinct models for k_{-1}^{∞} were used to match the experimental value[31] in the simulations. The energy transfer parameter α for argon collider gas was varied systematically until reasonable agreement with the experimental falloff curve at 297 K was obtained. The parameters are summarized in Tables 3 and 4 and the simulated falloff plots are compared with the experimental results in Figure 3.

The four models can all be made to agree reasonably well with the experimental data, as shown in Figure 3. All four models were constrained to match the value for k_{-1}^{∞} reported by Wollenhaupt and Crowley, which leads to rate constant simulations that appear to be a little low at higher pressures. All four models give fits of comparable quality when used with corresponding values for energy transfer parameter α for argon collider, even though the models themselves are distinctly different. Note however that the values of α range from ∼250 to ∼2000 cm^{-1}.

An additional test of the model was carried out by simulating the experiments of Scholtens et al.,[47] who recently determined

an improved upper limit to the CH_3ONO_2 yield in reaction B in N_2 collider gas. The test consisted of using the L−J model for the loose transition states and the ILT model for the isomerization reaction (with $A_\infty = 1 \times 10^{17}$ s^{-1} and $E_0 = 48$ kJ mol^{-1}). This critical energy for the isomerization reaction was chosen to be 2.5 kJ mol^{-1} below the threshold for reaction 3, in rough accord with the isomerization transition state for the R = OH• system reported by Dixon et al.,[39] which is at a much more accessible energy than the transition state found by Ellison et al.[41] The A-factor was chosen to correspond to a transition state that is much looser than the norm, but tighter than that for reaction (−2). Using this model, the yield of CH_3ONO_2 was found to be ∼0.05%, easily in agreement with the upper limit of <3% determined by Scholtens et al.[47]

The model simulations support an important conclusion: the magnitude of energy transfer parameter α depends sensitively on the assumed properties of the loose transition state. Since the properties of the transition state are not known with any certainty, α is merely a fitting parameter and its value cannot be compared quantitatively with values measured by direct energy transfer experiments. Furthermore, these results show that differences between "direct" energy transfer measurements and energy transfer parameters deduced from competitive chemical measurements involving loose transition states may be due largely to the arbitrary choice of transition state parameters. Some of this difficulty may be obviated if variational transition state theory[8,18] is used with an accurate potential energy surface. Unfortunately, obtaining a potential energy surface of sufficient accuracy is both difficult and expensive.[39,48,49]

A second conclusion is that energy transfer in the CH_3ONO_2 system is of the same order as in the $HONO_2$ system. Except for substitution of H for CH_3, the reaction of OH• with NO_2 is very similar to the reaction involving CH_3O•. In the HNO_3 system with a restricted Gorin transition state based on the L−J potential energy obtained in the same way as that described here, the value obtained for α with N_2 collider gas is ∼500 cm^{-1}.[33] Nitrogen is usually comparable in collision efficiency to argon;[42,50−53] hence, one expects α for CH_3ONO_2 with argon collider to be about the same for $HONO_2$ with N_2 collider. This prediction is only roughly confirmed, since it was found here that α ≈ 1000 cm^{-1} for the L−J restricted Gorin model for CH_3O• + NO_2 in argon. Since the restricted Gorin models are rather arbitrary, the prediction is not strong, but it leads us to expect that energy transfer in systems involving larger alkyl groups will have comparable energy transfer parameters (see discussions in refs 42, 51, 52, and 54 of the transferability of energy transfer parameters).

2-$C_5H_{11}O_2$• + NO → Products. This reaction system is modeled as described above by varying the energy transfer parameter α and the isomerization reaction parameters (A-factor and energy barrier). For $C_5H_{11}ONO_2$, the combined yields expressed as $k_A/(k_A + k_B)$ of 2- and 3-$C_5H_{11}ONO_2$ are reported as functions of both temperature (284−341 K) and of pressures up to 740 Torr of synthetic air,[6,55] as shown in Figure 4. In a more recent paper, separate yields of 2- and 3-$C_5H_{11}ONO_2$ are reported and are shown to agree well with the combined yields reported earlier. Atkinson et al.[56,57] showed that the 2- and 3-$C_5H_{11}ONO_2$ are produced with yields of 0.106 and 0.126, respectively, near 300 K and one atmosphere of air. Because the yields are so similar, we assume that 2- and 3-$C_5H_{11}ONO_2$ formation rate constants are the same and that the combined yield can be modeled using 2-$C_5H_{11}ONO_2$ alone.

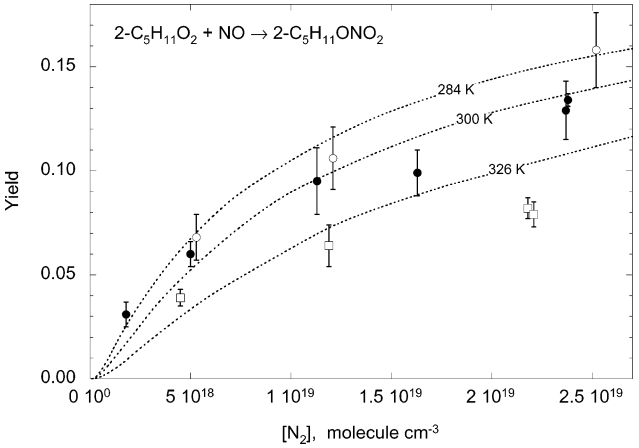

Figure 4. 2-Pentylnitrate yields as a function of temperature and nitrogen concentration. Data are from Atkinson et al.[55,58] and lines are model calculations from this work, assuming α = 25 cm^{-1}, $E_0 = 52.5$ kJ mol^{-1}, $A_\infty = 6.3 \times 10^{16}$ s^{-1}, and the parameters in Table 6 (see text for details).

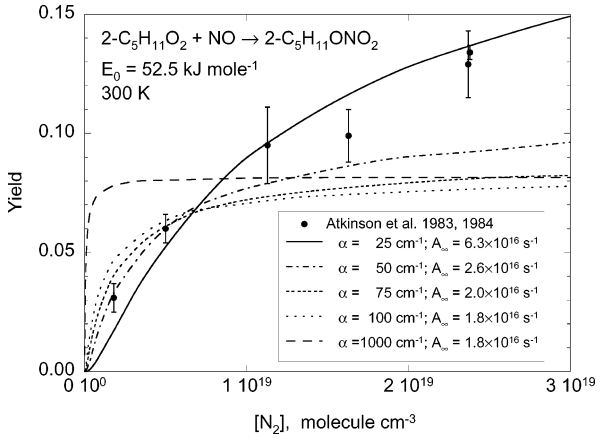

Figure 5. Yield of 2-$C_5H_{11}ONO_2$ at 300 K. Data (points) are from Atkinson et al.[55,58] Model calculations are based on the ILT model for the isomerization reaction with $E_0 = 52.5$ kJ mol^{-1} (see text and Table 6) and A-factors given in the figure legend.

Yields are first calculated for 2-$C_5H_{11}ONO_2$ at 300 K and two pressures, 200 and 800 Torr, at which the experimental yields are in the ratio of 1/2.[55] Calculations are performed first by assuming a relatively high critical energy for the isomerization reaction and systematically varying the energy transfer parameter α and A_3, the isomerization reaction A-factor. For these calculations, the isomerization activation barrier was arbitrarily chosen to be 52.5 kJ mol^{-1}, an energy ∼k_BT in energy below the critical energy for reaction 2. Results obtained with α ranging from 25 to 1000 cm^{-1} are presented in Figure 5. These results show that to match the shape of the experimental pressure dependence requires α ≈ 25 cm^{-1}. Similar results are obtained for assumed critical energies ranging down to 20 kJ mol^{-1}, as shown in Figure 6. Good agreement with experiment is obtained as long as A_3 is related to E_0 according to $A_3/\text{s}^{-1} \approx 1 \times 10^{12} \exp(0.21E_0/\text{kJ mol}^{-1})$. These results show that the energy transfer parameter α is closely correlated to E_0 and the data are not sensitive to particular values of E_0.

Yields were also calculated for 2-$C_5H_{11}ONO_2$ at 284, 300, and 326 K as a function of nitrogen concentration, for comparison with the experimental data[55,58] (Figure 4). The temperature-dependent recombination rate constants[27−29] were used to constrain the high-pressure limit unimolecular rate constants, as described above. The energy-dependent $k(E)$'s for the dissociation reactions were calculated using restricted Gorin

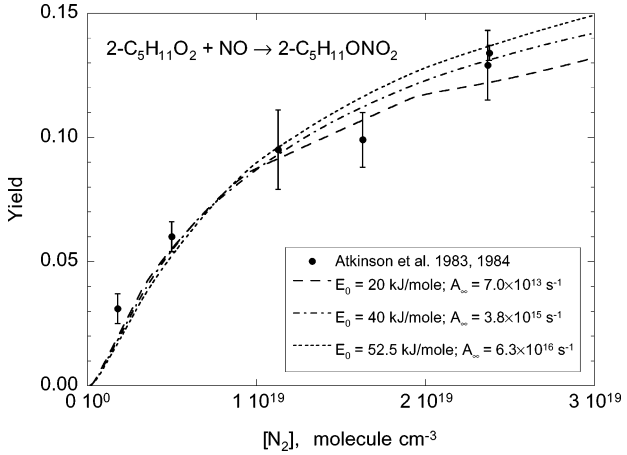

Figure 6. Yield of 2-$C_5H_{11}ONO_2$ at 300 K in N_2 bath gas. Data (points) are from Atkinson et al.[55,58] Model calculations are based on the ILT model for the isomerization reaction with energy transfer parameter $\alpha = 25$ cm^{-1} (see text and Table 6).

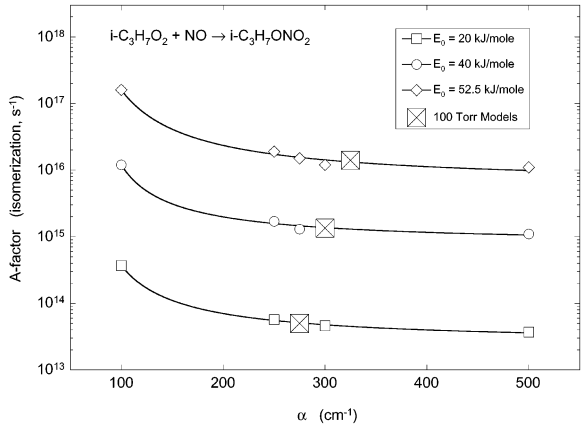

Figure 7. Acceptable models for *i*-$C_3H_7ONO_2$ relative yields[6,57] of 0.04 at 296 K and 750 Torr of N_2 (also see Table 5). Also shown are models that produce relative yields[59] of 0.006 at 100 Torr of N_2.

models, based on the Lennard−Jones interaction potential, as described above. Moments of inertia and hindrance information for the models are summarized in Table 6. The ILT method was used to describe the isomerization reaction by assuming $A_3 = 6.3 \times 10^{16}$ s^{-1} and $E_0 = 52.5$ kJ mol^{-1}, parameters that were shown above to give very good agreement with the experimental data at 300 K. The energy transfer parameter $\alpha = 25$ cm^{-1} was assumed. In Figure 4, the calculations show very good agreement with the experimental data at 284 and 300 K, and satisfactory agreement at 326 K.

***i*-$C_3H_7O_2$• + NO → *i*-$C_3H_7ONO_2$.** For *i*-$C_3H_7ONO_2$, the experimental yield expressed as $k_A/(k_A + k_B) = 0.039 \pm 0.005$ has been reported for 299 K and 735 Torr of synthetic air.[6,57] At 298 K and 100 Torr of N_2 the yield is reported to be 0.006 ± 0.003.[59] The reaction yields of *i*-$C_3H_7ONO_2$ are calculated in the same way as those for 2-$C_5H_{11}ONO_2$. Representative models that fit the experimental datum at 735 Torr are presented in Figure 7 for energy transfer parameter α ranging from 100 to 500 cm^{-1}, and isomerization critical energies of 20, 40, and 52.5 kJ mol^{-1}. It is noteworthy that for $\alpha \leq 75$ cm^{-1}, it is not possible to match the 735 Torr experimental yield. Also shown in Figure 7 are three models that fit the 735 Torr[6,57] and 100 Torr[59] experimental data simultaneously. In all three cases, the energy transfer parameter $\alpha \approx 300$ cm^{-1}. Considering the reported uncertainty[59] in the lower pressure yields, the resulting uncertainty in the energy transfer parameter α is of the order of $\sim$100 cm^{-1}. In any event, the energy transfer parameters

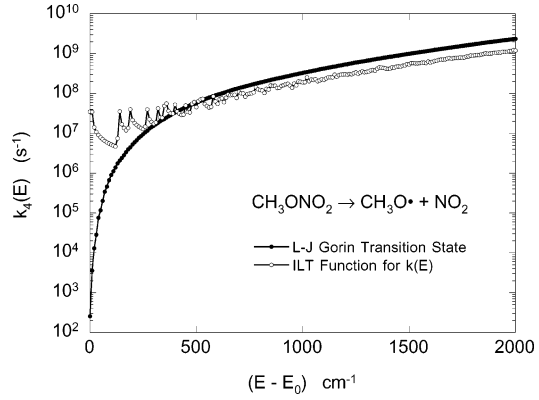

Figure 8. $k(E)$ from RRKM theory with the L−J hindered Gorin model compared to $k(E)$ from the ILT expression for reaction 4 with R = CH_3.

that are consistent with these data for R = *i*-C_3H_7 are reasonably consistent with those for R = H and R = CH_3, which were discussed above.

CH_3ONO_2 → HONO + CH_2O. Nitrous acid (HONO) is a known product of the reaction between CH_3O• and NO_2.[29−31,37] McCaulley et al.[37] concluded that the HONO produced from CH_3O• + NO_2 was due to a second-order metathesis reaction that is separate from the recombination reaction. In the preceding companion paper in this issue, we report finding a five-center cyclic transition state for the concerted elimination of HONO from CH_3ONO_2. From the vibrational frequencies and structure of the transition state, we calculate that the A-factor for the five-center reaction is $A_\infty = 3.5 \times 10^{12}$ s^{-1}, in reasonable accord with experimental values for similar reactions.[3]

The calculated reaction barrier height is not expected to be very accurate, and so it is useful to consider two limiting cases. Case 1: energy barrier comparable to, or greater than, the CH_3O-NO_2 dissociation energy and case 2: energy barrier much lower than the dissociation energy. For case 1, A_4 is more than 10^4 times as large as that for HONO elimination. Therefore, HONO elimination will not be significant if the barrier is relatively high.

If the barrier is very low (case 2) and the HONO elimination reaction is fast, then recombination of CH_3O• with NO_2 will result in HONO elimination to the exclusion of redissociation. If redissociation does not take place, then the CH_3O• kinetics will show no pressure falloff, contrary to the reported measurements. Therefore, we conclude that HONO elimination is not important and can be neglected in the models.

Discussion

It is clear from the results described above that the reaction scheme can describe all of the experimental results for R = CH_3, *i*-C_3H_7, and 2-C_5H_{11}. Although the detailed models are not greatly constrained, it is important to understand the features that are common to all of the models and those that are different.

Energy Transfer. For R = CH_3, a wide range of models for reaction (−4) can fit the results, but the different models require very different energy transfer parameters. Consider the restricted Gorin model and the ILT model with the same critical energy. According to RRKM theory, the only difference between the two transition state models is found in the respective sums of states ($G^{\ddagger}(E-E_0)$ in eq 1). Each model is plausible, although the restricted Gorin model is more appropriate for a loose transition state.[3,13,19] Both models give the same value for k_∞ at 296 K. But the two models produce $k(E)$'s near the threshold that differ significantly, as shown in Figure 8. As a result of

the different $k(E)$ functions, the initial energy distributions differ slightly (see eq 5) and different energy transfer parameters are needed in order to match the experimental falloff data shown in Figure 4.

Good fits to the experimental data can be achieved with many different models because neither the transition state model nor the energy transfer parameters are known independently: errors in one can compensate for errors in the other. Thus, an important conclusion is that if the transition state model is not well-known, then reaction rate studies are not good sources of absolute magnitudes of the energy transfer parameter α. Generally, reactions with fixed transition states are better sources of energy transfer parameters than reactions with loose transition states.

Although the absolute magnitude of energy transfer parameter α cannot be obtained from models where the transition state is not well-known, there is an indication that α can be transferred from one system to another when the assumed transition states are very similar. For example, the transition states for reaction (−4) when R = H, CH_3, and *i*-C_3H_7 are very similar loose transition states.[33] When the transition states are approximated as similar restricted Gorin models based on the Lennard−Jones interaction potential, the resulting values for α are ∼500, ∼1000, and ∼300 cm^{-1} for R = H, CH_3, and *i*-C_3H_7, respectively. Assuming the experimental data are correct, this variation shows that although α cannot be transferred simply from one system to another, it varies over only a relatively limited range.

In the present work, all of the loose transition states for R = 2-C_5H_{11} are restricted Gorin models constructed as described above and based on the Lennard−Jones interaction potential. Thus, we anticipated finding $\alpha \approx 500$ cm^{-1} in this system, within a factor of 3−5. Instead, we find the best fit with $\alpha \approx 25$ cm^{-1}, which is only 1/20 of the expected value. Note that for R = H and CH_3, the information needed to determine α is derived from falloff data for reaction (−4), while for R = *i*-C_3H_7, yield data from the full chemical activation system provide the information. The very large discrepancy between the anticipated value and the best fit value in the case of 2-C_5H_{11} may be due to erroneous assumptions made in constructing the models, or to erroneous experimental data. It is unlikely that the floppy R = 2-$C_5H_{11}ONO_2$ species are less easily deactivated than the more rigid cases (R = H, CH_3, and *i*-C_3H_7), because laboratory data for hydrocarbon species[53,60] and classical trajectory calculations[61−63] indicate that the presence of internal rotors and low-frequency vibrations tend to facilitate collisional energy transfer.[42]

Mechanics of Reaction B. With all of the models we have described here, the reactive flux enters according to reaction 1 and produces excited ROONO*, which can dissociate according to reaction 2, or isomerize according to reaction 3. The rates of reactions (−1) and (−3) are negligible, compared to the other reactions. Reaction 2 is not only very fast, but its rate constant is highly constrained by the known rate constant for reaction (−2). Thus, the lifetime of the excited ROONO* cannot be longer than dictated by reaction 2. Energy-dependent specific $k(E)$'s for reactions 2−4 are shown in Figure 9 as functions of vibrational energy. At one atmosphere, the collision frequency is $\sim 10^{10}$ s^{-1} and it is clear from the figure that the lifetime of excited ROONO* is too short for significant collisional deactivation to take place prior to reaction, even if reaction 3 is neglected. Thus significant collisional deactivation can only affect the highly excited $RONO_2$* produced by reaction 3.

For energy transfer parameter α similar in magnitude to that found from RO• + NO_2 falloff with R = CH_3 and OH, collisional deactivation of excited 2-$C_5H_{11}ONO_2$* is very

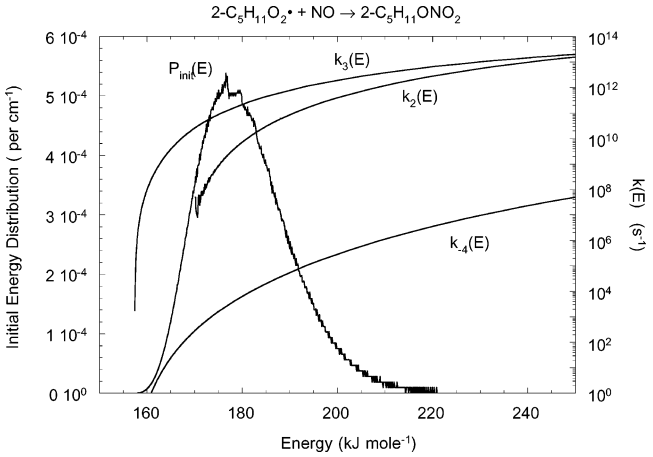

Figure 9. Unimolecular specific rate constants ($k(E)$'s, endothermic direction) and initial (chemical activation) energy distribution.

efficient, because of the long lifetime of the nascent molecules. According to Figure 9, the rate constant for $RONO_2$* decomposition via reaction 4 is of the order of 10^4 s^{-1}, which is far slower than collision frequency at one atmosphere ($\sim 10^{10}$ s^{-1}). With energy transfer parameters of the order of $\alpha = 1000$ cm^{-1}, collisional stabilization is highly efficient, producing large yields of stabilized $RONO_2$ even at relatively low pressures. Under those conditions, the yields of alkyl nitrates are controlled by the ratio $k_3(E)/[k_3(E) + k_2(E)]$, averaged over the energy distribution, and the yield is practically constant at pressures greater than ∼100 Torr, as shown in Figure 5.

The reported alkyl nitrate yields continue to increase even when the pressure approaches one atmosphere. With the models described here, excited ROONO* experiences essentially no collisions during its lifetime and, hence, is not responsible for the pressure dependence of the alkyl nitrate yields. Therefore, collisional deactivation of $RONO_2$* must be responsible. A fit to the experimental pressure dependence can only be achieved if the collisional deactivation of excited $RONO_2$* is extremely inefficient. The model calculations give the best fit for $\alpha \approx 25$ cm^{-1}, which is only about 12% of k_BT at 300 K. For such a small value of α, the population distribution of excited $RONO_2$* tends to broaden with time, in addition to cascading down the energy ladder, because activating collisions are nearly as effective as deactivating ones. Because most of the excited molecules are deactivated very slowly, decomposition via reaction 4 competes very effectively. The result is a small, pressure-dependent yield of alkyl nitrate.

The energy transfer parameters for deactivation of $RONO_2$* that are deduced from the alkyl nitrate yields are exceptionally small. Physical measurements of toluene deactivation[42,53] would give 270 cm^{-1} (for N_2 collider gas) at the same internal energy, which can be compared with ∼500 cm^{-1} obtained for $HONO_2$ (Golden et al.[33]) and ∼1000 and ∼300 cm^{-1} obtained in this work for CH_3ONO_2 and *i*-$C_3H_7ONO_2$, respectively. As was shown above, the properties of the loose transition states are not independently constrained and errors in the transition state can compensate for errors in α (and vice versa). As a result, the value of α may vary over a wide range, depending on assumed transition state parameters, perhaps accounting for the difference between the estimate based on physical methods and those obtained from fitting the RO• + NO_2 reaction data. Nevertheless, the value of α obtained from the alkyl nitrate yields is exceptionally small, especially since there is an indication that values of α are transferable between systems where the transition states are formulated in the same way (see

above). This exceptionally small value of α may signal that there are errors in the pressure-dependent data for alkyl nitrate formation, or that there are important errors or omissions in the model presented here.

Several aspects of the model presented here can be examined further. For example, all of the collisional effects are centered on $RONO_2$* and not on ROONO*. To develop a model in which ROONO* can be collisionally deactivated would require that its lifetime be much longer. However, there are strong constraints on this lifetime. The recombination rate constant for reaction (−2) provides a strong constraint on the rate of reaction 2, if the equilibrium constant is known. The equilibrium constant depends very strongly on the thermochemistry of ROONO and less strongly on its vibrational frequencies and molecular structure. Both the thermochemistry and molecular properties of ROONO are calculated with robust consistency by ab initio and DFT electronic structure methods,[7] and the results are in good agreement with experimental data for HOONO.[32] To increase the lifetime of 2-C_5H_{11}OONO by a factor of 100 would require that the 2-C_5H_{11}O−ONO bond dissociation energy be increased by ∼25 kJ mol^{-1}, a change much greater than the small differences that come about from using different electronic structure methods. Thus, the constraints on the lifetime of ROONO* appear to be strong, and collisional deactivation of this species is unlikely to be important for R ≤ C_5H_{11}.

The present model is based on statistical RRKM theory for reaction. If statistical rate theory is not appropriate, is it possible to have a model with larger values of the energy transfer parameter? The breakdown of statistical theory comes about when intramolecular vibrational energy redistribution (IVR) has a characteristic rate on the same order as the unimolecular rate,[64−66] and it may apply to either (or both) ROONO* and $RONO_2$*. In the case of ROONO*, most of the chemical energy release is initially localized in the new OO−NO bond, and slow IVR will leave ROONO* with excess energy localized in the OONO moiety. However, it is the OONO moiety in which the RO−ONO dissociation occurs. Therefore, slow IVR will result in even *shorter* lifetimes for ROONO* and hence even *less* chance of collisional deactivation.

For $RONO_2$*, a different effect is expected. Following isomerization, the energy will be localized in the ONO_2 moiety, which will enhance the O−NO_2 bond fission rate. With a faster rate constant for bond fission, larger values for α will be needed to stabilize the excited species. If the rate of reaction 4 is enhanced by a factor of 100−1000 (producing $k_4(E)$ of the order of 10^8−10^9 s^{-1}), then values for α will be more similar to the expected values. However, if the IVR rates are of roughly the same order as $k_4(E)$, they would be anomalously slow. Furthermore, there is no indication of unusual effects in the OH• and CH_3O• + NO_2 systems, which are at lower vibrational energy and which have smaller substituents, where one would expect IVR to be even slower. Therefore, if IVR in $RONO_2$* is anomalously slow, then that could explain the surprisingly small values of α found in our present model calculations. However, there is no experimental or theoretical evidence for such anomalously slow IVR rates, even in similar systems.

Is the model for the isomerization reaction reasonable? The isomerization reaction A-factors for the R = 2-C_5H_{11} models with α = 25 cm^{-1} vary over a very wide range, depending on the assumed critical energies (Figure 6). In the HOONO system, Dixon et al. found an isomerization transition state with critical energy near the HO−ONO dissociation energy.[39] They characterized the transition state as resembling loosely bound OH• and NO_2. By analogy, we assume that the isomerization reaction has a threshold at 52.5 kJ mol^{-1} (2.5 kJ mol^{-1} below the RO−ONO dissociation energy). The corresponding A-factor that gives good agreement with the experimental yields is $A_3 = 6.3 \times 10^{16}$ s^{-1} (see Figure 5), which is about one-third of the A-factor for the RO−ONO dissociation: $A_4 = 2.1 \times 10^{17}$ s^{-1} (see Table 6). Thus, the isomerization transition state according to this model is only slightly tighter than the loose transition state for bond fission. This result is also consistent with the transition state found by Ellison et al.,[41] which has a higher energy (near the energy of RO_2• + NO), but is very loose, with an A-factor of ∼10^{17} s^{-1} (calculated by us from vibrational frequencies and structure communicated by G. B. Ellison and J. F. Stanton). Whether the isomerization occurs during a near-dissociation of weakly bound RO−ONO,[39] or near a crease in the potential energy surface,[41] this three-center cyclic isomerization is qualitatively very different from the much tighter transition states calculated[67] for 1,2-hydrogen shifts in alkyl radicals, which have energy barriers of ∼160 kJ mol^{-1} and A-factors of ∼10^{13} s^{-1}.

It is possible that the pressure-dependent experimental data are in error. Numerous researchers have demonstrated that alkyl nitrates are formed via reaction B. Several experimental techniques have been used to detect alkyl nitrates, including gas chromatography with flame ionization or electron capture detectors, Fourier Transform Infrared spectroscopy, chemical ionization mass spectrometry, and other methods, as summarized in review articles.[2,4,5] However, only two systematic studies of pressure-dependent alkyl nitrate yields have been carried out, and both of those studies were carried out in the same laboratory with the same experimental technique (gas chromatography).[55,68] Although the data from those studies appear to be of high quality and show no signs of experimental defects, the difficulty we have encountered in attempting to model this system compels us to recommend that additional measurements be carried out using a variety of experimental techniques. If new experiments produce significantly different results, then the modeling of this system should be revisited. If new experiments confirm the old ones, then that will be a clear signal that the conventional model for this system requires substantial revisions. If conventional models with large values of α are correct, then we predict that the 2-pentylnitrate yields will be essentially independent of pressure for pressures greater than ∼100 Torr.

The conventional models for this system could be improved significantly if either (or both) the transition state properties can be characterized accurately and the energy transfer is better understood. Better characterization of either of these aspects would constrain the model much more strongly and help in identifying its deficiencies. Better characterization of energy transfer would require a reliable theory for the process, but there is none, except for classical trajectory calculations, which require accurate potential energy surfaces.[42] Better characterization of the transition states would require variational transition state calculations based on accurate multi-configuration electronic structure calculations, which are very challenging and expensive for systems of this size and complexity (see the preceding companion paper in this issue). In the present work (including the preceding companion paper), we consider only the singlet electronic state. It is possible that reactions on the triplet potential energy surface can play a role in this system. More extensive calculations would be needed to calculate the triplet potential surface and assess its role, if any.

Conclusions

It is shown in this work that master equation models can give very good descriptions of alkyl nitrate yields in three individual

systems: $CH_3O\bullet + NO_2$, $i\text{-}C_3H_7O_2\bullet + NO$, and $2\text{-}C_5H_{11}O_2\bullet + NO$. However, the energy transfer parameters deduced in the first two systems are very different from that deduced in the third system. Although the master equation models are constrained in several ways, it is found that variations in assumed properties of the isomerization reaction can be compensated essentially completely by variations in the assumed energy transfer. The prospects for a predictive model are not promising at this time.

Improvements will come only at significant cost. The models can be improved by carrying out challenging calculations to constrain the transition state properties and to assess the effects of triplet states in this system. Independent information on energy transfer would also be very useful. Of highest priority, however, is the need to reinvestigate the pressure-dependence of the alkyl nitrate yields by using a variety of experimental techniques. The models depend directly on the accuracy of the limited experimental data that are currently available. New experiments can validate, or replace the current data set, leading to new models that may be useful for predictions.

Acknowledgment. This project has been supported in part by the American Chemistry Council (through its Atmospheric Chemistry Technical Implementation Panel, contract #0092) and the National Science Foundation (Atmospheric Chemistry Division). The authors particularly thank Timothy J. Wallington for discussions and for a survey of the literature. They also thank Theodore S. Dibble and Joseph S. Francisco for helpful discussions and for sharing computational results. Thanks go to G. Barney Ellison and John F. Stanton for a preprint of their paper and for communicating their results prior to publication, and to M. C. Lin for a preprint of his paper with R. S. Zhu. Thanks also go to David M. Golden, Neil Donahue, Geoffrey Tyndall, and John Orlando for discussions. S.R. thanks the Undergraduate Research Opportunities Program at the University of Michigan for support.

Supporting Information Available: Tables of vibrational frequencies and moments of inertia for R = CH_3, $i\text{-}C_3H_7$, $2\text{-}C_5H_{11}$, and NO_x. This material is available free of charge via the Internet at http://pubs.acs.org.

References and Notes

(1) Darnall, K. R.; Carter, W. P. L.; Winer, A. M.; Lloyd, A. C.; Pitts, J. N. *J. Phys. Chem.* **1976**, *80*, 1948−50.
(2) Lightfoot, P. D.; Cox, R. A.; Crowley, J. N.; Destriau, M.; Hayman, G. D.; Jenkin, M. E.; Moortgat, G. K.; Zabel, F. *Atmos. Environ.* **1992**, *26A*, 1805−961.
(3) Benson, S. W. *Thermochemical Kinetics*, 2nd ed.; Wiley: New York, 1976.
(4) Roberts, J. M. *Atmos. Environ.* **1990**, *24A*, 243−87.
(5) Wallington, T. J.; Nielsen, O. J.; Sehested, J. Reactions of organic peroxy radicals in the gas phase. In *Peroxyl Radicals*; Alfassi, Z. B., Ed.; John Wiley & Sons: Chichester, UK, 1997; pp 113−72.
(6) Atkinson, R.; Aschmann, S. M.; Carter, P. L.; Pitts, J. N., Jr. *J. Phys. Chem.* **1982**, *86*, 4563−9.
(7) Lohr, L. L.; Barker, J. R.; Shroll, R. M. *J. Phys. Chem. A* **2003**, *107*, 7429.
(8) Zhang, D.; Zhang, R.; Park, J.; North, S. W. *J. Am. Chem. Soc.* **2002**, *124*, 9600−5.
(9) Forst, W. *Theory of Unimolecular Reactions*; Academic Press: New York, 1973.
(10) Barker, J. R. *Int. J. Chem. Kinet.* **2001**, *33*, 232−45.
(11) Barker, J. R.; Ortiz, N. F. *Int. J. Chem. Kinet.* **2001**, *33*, 246−61.
(12) Barker, J. R. MultiWell Program Suite (1.3.2); 1.3.2 ed.; http://aoss.engin.umich.edu/multiwell/, Ann Arbor, MI, 2003.
(13) Gilbert, R. G.; Smith, S. C. *Theory of Unimolecular and Recombination Reactions*; Blackwell Scientific: Oxford, 1990.
(14) Robinson, P. J.; Holbrook, K. A. *Unimolecular Reactions*; Wiley-Interscience: New York, 1972.
(15) Beyer, T.; Swinehart, D. F. *Comm. Assoc. Comput. Machines* **1973**, *16*, 379.
(16) Stein, S. E.; Rabinovitch, B. S. *J. Chem. Phys.* **1973**, *58*, 2438−45.
(17) Forst, W. *J. Phys. Chem.* **1972**, *76*, 342.
(18) Truhlar, D. G.; Garrett, B. C. *Acc. Chem. Res.* **1980**, *13*, 440−8.
(19) Smith, G. P.; Golden, D. M. *Int. J. Chem. Kinet.* **1978**, *10*, 489.
(20) Gorin, E. *Acta Physicochim., URSS* **1938**, *9*, 691.
(21) Varshni, V. P. *Rev. Mod. Phys.* **1957**, *29*, 664−82.
(22) Klippenstein, S. J.; Khundkar, L. R.; Zewail, A. H.; Marcus, R. A. *J. Chem. Phys.* **1988**, *89*, 4761−70.
(23) Miller, J. A.; Klippenstein, S. J. *J. Phys. Chem. A* **2000**, *104*, 2061−9.
(24) Duchovic, R. J.; Hase, W. L. *Chem. Phys. Lett.* **1984**, *110*, 474−7.
(25) Huber, K. P.; Herzberg, G. *Molecular Spectra and Molecular Structure. IV. Constants of Diatomic Molecules*; Van Nostrand Reinhold Co.: New York, 1979.
(26) Herzberg, G. *Molecular Spectra and Molecular Structure. III. Electronic Spectra and Electronic Structure of Polyatomic Molecules*, 2nd ed.; Van Nostrand Reinhold Co.: Cincinnati, 1966.
(27) Atkinson, R. *J. Phys. Chem. Ref. Data* **1994**, *Monograph No. 2*.
(28) Atkinson, R. *Atmos. Environ.* **2000**, *34*, 2063−101.
(29) Atkinson, R.; Baulch, D. L.; Cox, R. A.; R. F. Hampson, J.; Kerr, J. A.; Rossi, M. J.; Troe, J. *J. Phys. Chem. Ref. Data* **2000**, *29*, 167−266.
(30) DeMore, W. B.; Sander, S. P.; Golden, D. M.; Hampson, R. F.; Kurylo, M. J.; Howard, C. J.; Ravishankara, A. R.; Kolb, C. E.; Molina, M. J. Chemical Kinetics and Photochemical Data for Use in Stratospheric Modeling. Evaluation Number 12, Jet Propulsion Laboratory, 1997.
(31) Wollenhaupt, M.; Crowley, J. N. *J. Phys. Chem. A* **2000**, *104*, 6429−38.
(32) Hippler, H.; Nasterlack, S.; Striebel, F. *Phys. Chem. Chem. Phys.* **2002**, *4*, 2959−64.
(33) Golden, D. M.; Barker, J. R.; Lohr, L. L. *J. Phys. Chem. A* **2003**, submitted for publication.
(34) Golden, D. M.; Smith, G. P. *J. Phys. Chem. A* **2000**, *104*, 3991−7.
(35) Biggs, P.; Canosa-Mas, C. E.; Fracheboud, J.-M.; Parr, A. D.; Smallcross, D. E.; Wayne, R. P. *J. C. S. Faraday Trans.* **1993**, *89*, 4163.
(36) Frost, M. J.; Smith, I. W. M. *J. C. S. Faraday Trans.* **1990**, *86*, 1757.
(37) McCaulley, J. A.; Anderson, S. M.; Jeffries, J. B.; Kaufman, F. *Chem. Phys. Lett.* **1985**, *115*, 180−6.
(38) Sumathy, R.; Peyerimhoff, S. D. *J. Chem. Phys.* **1997**, *107*, 1872−80.
(39) Dixon, D. A.; Feller, D.; Zhan, C.-G.; Francisco, J. S. *J. Phys. Chem. A* **2002**, *106*, 3191−6.
(40) Zhu, R. S.; Lin, M. C. *J. Phys. Chem. A* **2003**, submitted, private communication.
(41) Ellison, G. B.; Blanksby, S. J.; Jochnowitz, E. B.; Stanton, J. F., to be published.
(42) Barker, J. R.; Yoder, L. M.; King, K. D. *J. Phys. Chem. A* **2001**, *105*, 796−809.
(43) Mourits, F. M.; Rummens, F. H. A. *Can. J. Chem.* **1977**, *55*, 3007.
(44) Stiel, L. I.; Thodos, G. *J. Chem. Eng. Data* **1962**, *7*, 234.
(45) Halkiadakis, E. A.; Bowrey, R. G. *Chem. Eng. Sci.* **1975**, *30*, 53.
(46) Joback, K. G.; Reid, R. C. *Chem. Eng. Comm.* **1987**, *57*, 233.
(47) Scholtens, K. W.; Messer, B. M.; Kappa, C. D.; Elrod, M. J. *J. Phys. Chem. A* **1999**, *103*, 4378−84.
(48) Dutta, A.; Sherrill, C. D. *J. Phys. Chem. A* **2003**, *118*, 1610−9.
(49) Kumaran, S. S.; Su, M.-C.; Lim, K. P.; Michael, J. V.; Wagner, A. F.; Harding, L. B.; Dixon, D. A. *J. Phys. Chem.* **1996**, *100*, 7541−9.
(50) Hippler, H.; Troe, J. Recent direct studies of collisional energy transfer on vibrationally excited molecules in the electronic ground state. In *Advances in Gas-Phase Photochemistry and Kinetics: Bimolecular Collisions*; Ashfold, M. N. R., Baggott, J. E., Eds.; The Royal Society of Chemistry: London, 1989; p 209.
(51) Tardy, D. C.; Rabinovitch, B. S. *Chem. Rev.* **1977**, *77*, 369.
(52) Oref, I.; Tardy, D. C. *Chem. Rev.* **1990**, *90*, 1407.
(53) Barker, J. R.; Toselli, B. M. *Int. Rev. Phys. Chem.* **1993**, *12*, 305−38.
(54) Hold, U.; Lenzer, T.; Luther, K.; Reihs, K.; Symonds, A. *Ber. Bunsen-Ges. Phys. Chem.* **1997**, *101*, 552.
(55) Atkinson, R.; Carter, W. P. L.; Winer, A. M. *J. Phys. Chem.* **1983**, *87*, 2012−8.
(56) Atkinson, R.; Kwok, E. S. C.; Arey, J.; Aschmann, S. M. *Faraday Discussions* **1995**, *100*, 23−37.
(57) Arey, J.; Aschmann, S. M.; Kwok, E. S. C.; Atkinson, R. *J. Phys. Chem. A* **2001**, *105*, 1020−7.
(58) Atkinson, R.; Aschmann, S. M.; Carter, W. P. L.; Winer, A. M.; Pitts, J. N. *Int. J. Chem. Kinet.* **1984**, *16*, 1085−101.
(59) Chow, J. M.; Miller, A. M.; Elrod, M. J. *J. Phys. Chem. A* **2003**, *107*, 3040−7.
(60) Toselli, B. M.; Brenner, J. D.; Yerram, M. L.; Chin, W. E.; King, K. D.; Barker, J. R. *J. Chem. Phys.* **1991**, *95*, 176.

(61) Lim, K. F. *J. Chem. Phys.* **1994**, *100*, 7385.
(62) Lim, K. F. *J. Chem. Phys.* **1994**, *101*, 8756.
(63) Linhananta, A.; Lim, K. F. *Phys. Chem. Chem. Phys.* **1999**, *1*, 3467−71.
(64) Oref, I.; Rabinovitch, B. S. *Acc. Chem. Res.* **1979**, *12*, 166−75.
(65) Meagher, J. F.; Chao, K.-J.; Barker, J. R.; Rabinovitch, B. S. *J. Phys. Chem.* **1974**, *78*, 2535.
(66) Rabinovitch, B. S.; Meagher, J. F.; Chao, K.-J.; Barker, J. R. *J. Chem. Phys.* **1974**, *60*, 2932.
(67) Viskolcz, B.; Lendvay, G.; Seres, L. *J. Phys. Chem. A* **1997**, *101*, 7119−27.
(68) Atkinson, R.; Aschmann, S. M.; Winer, A. M. *J. Atmos. Chem.* **1987**, *5*, 91−102.
(69) Barker, J. R.; Brenner, J. D.; Toselli, B. M. The Vibrational Deactivation of Large Molecules by Collisions and by Spontaneous Infrared Emission. In *Vibrational Energy Transfer Involving Large and Small Molecules*; Barker, J. R., Ed.; JAI Press Inc.: Greenwich, CT, 1995; Vol. 2B.